Journal of Molecular Structure 965 (2010) 56–64

Contents lists available at ScienceDirect

Journal of Molecular Structure

journal homepage: www.elsevier.com/locate/molstruc

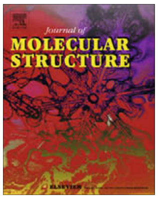

Synthesis and study of triorganostannyl esters of 3-,4- and 3,5-pyridinylimino substituted aminobenzoic acids: Crystal structures of dimorphs of aqua-trimethyltin 3-pyridinyliminobenzoate

Dimitris Tzimopoulos [a], Agnieszka Czapik [b], Maria Gdaniec [b,*], Thomas Bakas [c,*], Anvarhousein A. Isab [d], Anastasia-Catherine Varvogli [a], Pericles D. Akrivos [a,*]

[a] Department of Chemistry, Aristotle University of Thessaloniki, P.O.B. 135, 541 24 Thessaloniki, Greece
[b] Faculty of Chemistry, Adam Mickiewicz University, 60-780 Poznań, Poland
[c] Department of Chemistry, University of Ioannina, P.O.B. 1186, 451 10 Ioannina, Greece
[d] Department of Chemistry, King Fahd University of Petroleum and Minerals, Dhahran 31261, Saudi Arabia

ARTICLE INFO

Article history:
Received 24 August 2009
Received in revised form 30 October 2009
Accepted 17 November 2009
Available online 20 November 2009

Keywords:
Tin
Triorganotin carboxylates
X-ray diffraction
Mössbauer spectroscopy
NMR spectroscopy
MOPAC computations

ABSTRACT

The synthesis and the structural investigation of triorganostannyl esters of the 3- and 4-[1-pyridin-2-yl-methylidene]- and 3,5-bis-[1-pyridin-2-yl-methylidene]-benzoic acids are reported with methyl, *n*-butyl, cyclohexyl, phenyl and benzyl substituents on tin. The organic carboxylates may be considered as imino-pyridines emerging from the condensation of the corresponding aminobenzoic acid with pyridine-2-carboxaldehyde. In this respect it is interesting to investigate their physicochemical properties since their coordination to metal centers will affect both the photophysical properties of the metal and the conformation and intermolecular interactions of the ligands. Therefore, the structure of the above triorganotin compounds is studied and discussed in relation to those of the unsubstituted benzoates as well as of the free ligands. X-ray crystallography and a coalescence of spectroscopic methods applied both in the solid state and in solution have been used in this effort.

1. Introduction

Metal complexes of α-diimines reveal interesting electronic and optical properties and in this respect they have received much and detailed interest [1]. Substituted α-diimines offer the presence of more than one coordination site which may produce complex or unique structures and produce oligo or polymetallic systems with varying electronic and optical properties [2]. Vast numbers of coordination compounds are reported having in the coordination environment 2,2′-bipyridine, 9,10-phenanthroline or the condensation products of amine-bearing molecules with diacetyl, benzil and analogous compounds. Diimines produced from amino substituted benzoic acids have also been studied in this respect and to our knowledge have been used as the free acids to coordinate late transition metals in heteroleptic coordination compounds [3–5] through their diimine site.

Tuning the electronic effects of coordinated diimines has been attempted by many and is usually accomplished through substitution reactions at the ligand backbone. The carboxylate moiety in the Schiff bases synthesized from aminobenzoic acids and pyridine-2-carboxaldehyde is favoring the study of substitutions at this site and this is the starting point for our present study where we introduce a triorganotin residue to the carboxylic group. Triorganotin carboxylates are not a new group of compounds and in fact they have found a wide variety of applications including their action as pesticides, antifouling agents or cytostatic drugs [6], although their high toxicity has prohibited or halted their extensive use. Coordination of carboxylate to metals in general and to tin in particular offers the possibility of studying the variations of the coordination mode which include monodentate, chelate (symmetric or more often asymmetric) or the more subtle bridging which may produce oligomeric or polymeric compounds [7]. The energetic differences between the above modes of coordination are usually small and therefore it is not uncommon to observe more than one co-existing in the same crystal therefore giving rise to more complicated supramolecular structures.

Our current interest lies in the synthesis and study of the coordinating ability of triorganotin esters of aminobenzoate derivatives towards main group or transition metals. In this respect we are engaged in the synthesis of the pyridin-2-yl-methylidene substituted compounds which may act as iminopyridine donors to metal centers [8,9] and may prove to alter the metal site through changes in the organotin environment [10,11]. Concerning the tin environ-

---

* Corresponding author. Fax: +30 2310 997738.
E-mail address: akrivos@chem.auth.gr (P.D. Akrivos).

0022-2860/$ - see front matter © 2009 Elsevier B.V. All rights reserved.
doi:10.1016/j.molstruc.2009.11.038

ment the previous knowledge of the coordination behavior of the unsubstituted benzoates is valuable in correlating spectroscopic information with structure in the cases where the latter was not possible to be directly solved [12]. Semi-empirical computations are also used as an aid in the investigation of the electronic structure of the organic ligands and of the triorganotin derivatives and they ere found to be in general agreement with the known structures and observed spectroscopic data. Moreover, we describe the crystal structure of trimethyltin 3-[1-pyridin-2-yl-methylidene]-aminobenzoate hydrate in the two polymorphs it was isolated as well as those of two ligands, namely 3- and 4-[1-pyridin-2-yl-methylidene]-aminobenzoic acid. The substituted aminobenzoic acids utilized in the present study are presented in Fig. 2 and the general reaction scheme in summarized in Fig. 1.

2. Experimental

2.1. Materials and measurements

The triorganotin chlorides and the aminobenzoic acids were obtained from ACROS and were used without any further purification. The solvents used were of reagent grade and were not subjected to any further drying process prior to their use. Elemental analyses for C, H and N were performed on a Perkin-Elmer 240B elemental analyzer. Infrared spectra were recorded in KBr pellets on a Perkin-Elmer Spectrum One FTIR spectrometer with a resolution of 2 cm^{-1} following the collection of 16 scans over the range 4000–360 cm^{-1}. NMR for ^{1}H and ^{13}C were measured at 300 and 75 MHz, respectively, in $CDCl_3$ solutions on a Bruker 300 spectrometer using TMS as internal standard. Electronic excitation spectra were recorded in 1×10^{-4} M solutions in methanol and dichloromethane in 1 cm cuvettes on a Perkin-Elmer Spectrum One spectrometer and were processed with the Peakfit program at the Aristotle University central computing facility. Fluorescence measurements were carried out on the previous solutions or in the solid state in KBr pellets using a Hitachi F-7000 fluorescence spectrometer. The crystal structures were determined using a Kuma KM4CCD κ geometry diffractometer. Data collection and cell refinement were carried out with *CrysAlis CCD* [13] and data reduction with *CrysAlis RED* [13]; *SHELX-97* programs [14] were used to solve and refine the structure. Molecular graphics were generated with ORTEP-III for Windows [15] and Mercury 1.4 software [16]. CCDC 739745–739748 contain the supplementary crystallographic data for this paper. These data can be obtained free of charge via http://www.ccdc.cam.ac.uk/conts/retrieving.html (or from the Cambridge Crystallographic Data Centre, 12, Union Road, Cambridge CB2 1EZ, UK; fax: +44 1223 336033).

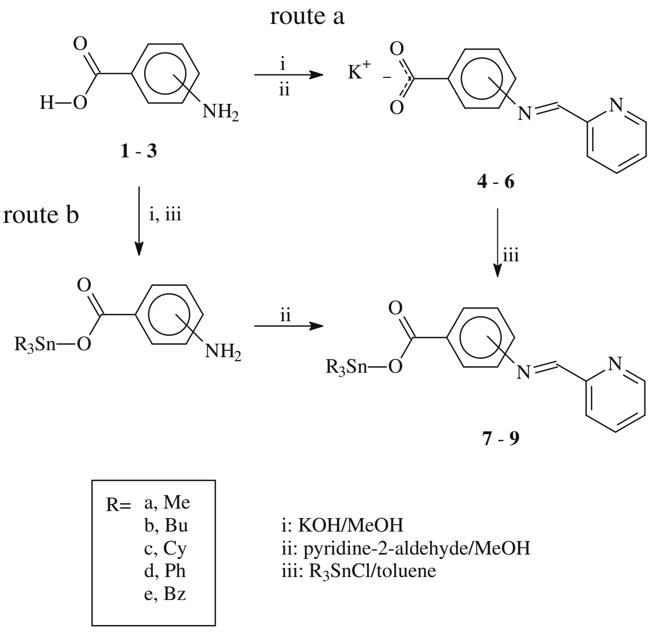

Fig. 1. General reaction scheme followed. The numbering of compounds corresponds to 3- (**4**, **7**), 4- (**5**, **8**) and 3,5- (**6**, **9**) substituted benzoic acids, respectively.

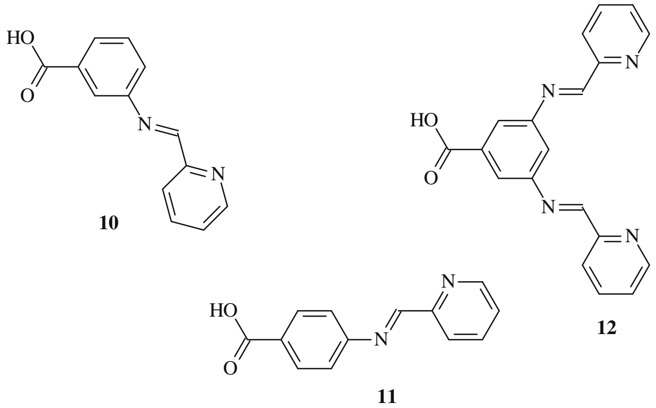

Fig. 2. Representation of the ligands synthesized and used in the present study.

Mössbauer spectra were obtained on powder samples at 80 K, using a constant acceleration spectrometer and a 10-mCi calcium stannate source kept at room temperature. Spectrometer calibration was effected using a metallic iron foil. Isomer shifts are reported relative to $CaSnO_3$, assuming that they are the same as the $BaSnO_3$ shifts.

2.2. Ligand synthesis

The general scheme for the synthesis of the triorganotin compounds is shown in Fig. 1. In general, “route a” was followed. However, for comparison reasons and especially for correlating spectroscopic data the imines themselves were synthesized, **10** and **11** according to literature method [3] with slight variations, which include the use of a single solvent (ethanol) and the avoidance of use of formic acid as catalyst. For **12** the following reaction procedure was adopted. To a suspension of of the acid (10.0 mmols) in methanol (10.0 mL) a solution of 2-pyridinecarboxaldehyde in methanol (5.0 mL) was added under stirring at room temperature. After the completion of the addition the mixture was refluxed for 1.5 h and then the grayish-yellow precipitate was collected by filtration, washed successively with cold ethanol, diethylether and finally dried in air.

2.3. Synthesis and characterization of the compounds

The imine salts of the parent acids were synthesized in the form of their potassium salts following the general route described below. 10.0 mmol of the appropriate potassium aminobenzoate were dissolved in methanol (10.0 mL) under stirring at room temperature. When dissolution was completed there was added pyridine-2-aldehyde (10.0 mmols) dissolved in methanol (5.0 mL) and the reaction was continued for a further 1.5 h under refluxing conditions. The solid product emerging (yellow for **5**, brownish-yellow for **4** and greyish for **6**) was filtrated through a Buchner funnel and washed with ethanol and diethylether before drying in air.

The triorganotin derivatives studied were prepared from the above salts without their prior isolation. At the end of the above procedure there were added to the mixture under continuous stirring 10.0 mmol of the appropriate triorganotin chloride in toluene (20.0 mL). The solution became clear instantly and was left to react under reflux for 5–6 h during which KCl deposited gradually on the vessel walls. The solution was then filtered while hot in order to remove the remaining KCl, the solvent was removed at the rotary evaporator and the solid (R = Me, Cy) or oily product (R = Bu, Ph, Bz) isolated was dried under vacuum. The products obtained were dissolved in the minimum amount of hot hexane-dichloromethane (10:1) and the precipitate formed upon cooling was filtrated and recrystallized from hot toluene–hexane (5:1).

The yellow or brownish-yellow products isolated in the case of the methyl derivatives were further dissolved in hot toluene and upon addition of petroleum ether the corresponding crystals used for X-ray determination were deposited for compound **7a**. In the case of the butyl and benzyl derivatives it proved necessary to use molecular sieves in order to avoid turpidity of the initial mixture and undesired by-products. For the compounds of the 3,5-disubstituted benzoic acid, the synthesis of the desired products was carried out after in the same manner but the refluxing periods had to be expanded to 3 and 8 h, respectively, for the two steps described previously. In the case of compound **7a**, upon standing at room temperature a light yellow solid deposited within minutes and was isolated and submitted for structural analysis which proved that it was actually the hydrate of **7a**. Upon further standing for a few days a second batch of crystals was deposited and these were also collected and analyzed in the same way, proving to be another polymorph of the same compound. Both structures are reported and they are denoted as polymorphs B and A of compound **7a**·H_2O, respectively. Selected crystallographic data are included in Table 5.

It should be noted at this point that the same products can be obtained by the interaction of the appropriate triporganostannyl esters of the aminobenzoates, prepared and isolated as described elsewhere [12] with a slight excess of pyridine-2-aldehyde in refluxing methanol for a period of 2 h.

The complexes were characterized spectrophotometrically (FTIR and UV–vis) and by elemental analysis; (theoretical values are shown in brackets):

10: C, 68.87% (69.02%); H, 4.73% (4.46%); N, 12.34% (12.38%); **11**: C, 68.42% (69.02%); H, 4.81% (4.46%); N, 12.06% (12.38%); **12**: C, 68.56% (69.08%); H, 4.54% (4.27%); N, 16.71% (16.96%); **7a**: C, 49.07% (49.40%); H, 4.67% (4.66%); N, 6.99% (7.20%); **8a**: C, 48.79% (49.40%); H, 4.70% (4.66%); N, 6.79% (7.20%); **9a**: C, 53.35% (53.58%); H, 4.50% (4.66%); N, 11.77% (11.36%); **7b**: C, 57.52% (58.27%); H, 7.16% (7.04%); N, 5.19% (5.44%); **8b**: C, 57.32% (58.27%); H, 7.18% (7.04%); N, 5.05% (5.44%); **9b**: C, 59.63% (60.11%); H, 6.97% (6.51%); N, 8.75% (9.05%); **7c**: C, 62.38% (62.75%); H, 7.30% (7.13%); N, 3.99% (4.72%); **8c**: C, 62.60% (62.75%); H, 7.49% (7.13%); N, 4.12% (4.72%); **9c**: C, 64.01% (63.71%); H, 6.74% (6.65%); N, 7.86% (8.03%); **7d**: C, 64.86% (64.73%); H,4.55% (4.21%); N, 4.38% (4.87%); **8d**: C, 64.55% (64.73%); H,4.50% (4.21%); N, 4.50% (4.87%); **9d**: C, 65.32% (65.40%); H,4.23% (4.15%); N, 8.33% (8.25%); **7e**: C, 65.78% (66.15%); H, 5.08% (4.90%); N, 4.43% (4.54%); **8e**: C, 65.92% (66.15%); H, 4.94% (4.90%); N, 4.68% (4.54%); **9e**: C, 66.08% (66.59%); H, 4.79% (4.75%); N, 7.63% (7.77%).

3. Results and discussion

3.1. Vibrational spectra

The structure adopted by organotin carboxylates is subtle since the coordination of the carboxylate ion may be monodentate, bridging or chelate. A compilation of spectroscopic evidence is needed in order to verify the coordination mode present in every case. In the IR spectrum the symmetric and asymmetric carboxylate stretching modes provide the widely accepted criterion of their spacing, $\Delta\nu$. Generally $\Delta\nu$ differences less than 240 cm^{-1} are accounting for bridging or chelating bonding modes while ones above 260 cm^{-1} for monodentate, [17]. In borderline cases and in absence of crystallographic evidence only speculations can be made, i.e. assumption o asymmetric bridging [18]. In addition, individual peak positions have been sporadically used as indication for the presence of specific coordination modes, i.e. the existence of a carboxylate band in the proximity of 1630 cm^{-1} is related to the asymmetric bridging of the carboxylate [19].

The relevant vibrational information for the ligands (**10**–**12**), their potassium salts (**4**–**6**) and the triorganotin derivatives (**7**–**9**) are reported in Table 1. The $\Delta\nu$ discussed above are also computed and tabulated in order to aid the interpretation of the carboxylate bonding mode.

The imine part of the ligands does not appear to take part in the coordination to tin because the corresponding bands do not sift from their position in the free ligands. Notable exceptions are **7b**, **7c** and **9a**. In the first two the strengthening of the C═N bond may be attributed to some twisting of the two rings of the ligand therefore precluding participation of the specific bond in any extended aromatic system. In the latter case the lower wavenumber of the bond stretching relative to the ligand may indicate a participation of the imine N atom in an interaction which may be either hydrogen-bond formation or coordination to tin. Regarding the coordination mode of the carboxylate moiety the trimethyltin derivatives **7a** and **8a** are proposed to be polymeric with carboxylate bridging adjacent tin centers while most of the rest compounds appear to have monodentate carboxylate. There exist a number of compounds, namely **7e**, **8e**, **9a** and **9c** for which no clear conclusion may be drawn; the compounds may be of polymeric nature like the trimethyltin derivatives discussed previously.

The above assignments for the asymmetric carboxylate and the imino C═N bond stretchings are aided by the known spectra of the corresponding unsubstituted benzoates [10,11,18,20] and by their correlation with the spectra of the studied compounds. Further support is provided by computations carried out on single molecules which were performed using the PM6 Hamiltonian [21] as implemented in the MOPAC2009 program [22]. Simple semi-empirical computations are not expected to result the accurate vibrational eigenvalues and there is always need for scaling in

Table 1
Relevant vibrational spectral data. Band maxima are given in wavenumbers.

Compound	$\nu_{as}(COO)$	$\nu_s(COO)$	$\Delta\nu$	$\nu(C{=}N)$	$\nu(Sn{-}O)$	$\nu(Sn{-}C)$
10	1703	1293	410	1628	–	–
4	1557	1395	162	1629	–	–
7a	1594	1374	220	1627	417	553
7b	1578	1332	246	1645	407	517
7c	1585	1328	257	1643	410	492
7d	1587	1333	254	1632	407	446
7e	1597	1335	232	1630	410	452
11	1701	1272	429	1629	–	–
5	1544	1403	141	1623	–	–
8a	1599	1367	232	1625	439	551
8b	1600	1338	262	1630	407	510
8c	1604	1315	289	1637	418	493
8d	1600	1331	269	1633	406	447
8e	1598	1366	232	1627	406	452
12	1704	1294	410	1635	–	–
6	1563	1390	173	1633	–	–
9a	1589	1338	251	1621	407	550
9b	1587	1331	256	1636	407	526
9c	1586	1326	250	1638	406	482
9d	1587	1331	256	1636	407	448
9e	1596	1332	267	1633	406	452

order to approach the experimental observations. However the correct ordering of the normal coordinate analysis cannot be overruled especially when it consistently determines higher frequencies for the C=O relative to the neighboring C=C and C=N bonds. In our case, both the free acids and their idealized triaryl and trialkyltin derivatives were studied by means of tight convergence criteria, i.e. setting the SCF convergence to 1.0×10^{-12} and the gradient norm to 0.01, respectively, for the geometry optimization which preceded the FORCE calculation.

Initially there is observed a coincidence of the computed and the crystallographically obtained molecular geometries for the ligands **10** and **11**. Both compounds are predicted to be non-planar due to a steric hindrance between the methylidene and benzene H atoms. Furthermore the carboxylate and imino region geometries are predicted reasonably close to the experimentally obtained ones although the computations assume an idealized gas-phase molecule with no intermolecular interactions and packing forces. C–O bond lengths are computed to be 1.209 and 1.380 Å (1.209 and 1.318 Å from X-ray data, *vide infra*) for compound **10** and 1.211 and 1.383 Å (1.212 and 1.329 Å X-ray) for compound **11**. The C-N bond lengths of the imino site are computed to be 1.428 and 1.294 Å (1.424 and 1.264 Å X-ray) for **10** while for **11** the values are 1.423 and 1.290 Å (1.415 and 1.273 Å X-ray), respectively.

The computations, in line with the intuitive assignment predict the C=O vibration to occur at the highest wavenumber with a very high consistency and a scaling factor of 0.932 while the imino C=N bond is predicted to follow. In the latter case however the scaling factor needed to be applied is 0.918. The vibrations computed appear to be strongly coupled to the stretches of the neighboring aromatic system. In both cases the ring C=C bonds are predicted to lie at lower wavenumbers.

3.2. Visible absorption spectra

The parent ligands and the triorganotin compounds synthesized reveal good solubility in a variety of organic solvents which made it possible to record their spectra in dichloromethane and methanol. The spectra of the ligands (Fig. 3) show some general similarities and some discrepancies which are due to the different solvating ability of the two solvents used. There is an apparent existence of at least five overlapping bands in every case, the position of which depends obviously on the solvent and on the ligand studied. This type of solvatochromism is expected in analogous aromatic systems. The analysis of the overlapping bands was carried out using the Peakfit program [23] within the AFS system of the Aristotle University of Thessaloniki [24]. The results of this analysis provided evidence for the occurrence of six bands in the recorded region most of which indicate, on grounds of both intensity and band half-width, a significant difference between the ground and excited states. Based on the good approximation of the molecular geometry obtained by the semi-empirical computations applied we proceeded with the investigation of the possible electronic excitations occurring within these molecules and we considered the single electron excitations involving the four higher occupied and the four lower occupied molecular orbitals, an approach incorporated into the MOPAC2009 package.

The frontier molecular orbitals for the two ligands are presented in Fig. 4 and 5. Among them there are orbitals localized mainly on the pyridine ring or bearing imino or carboxylate character as well, whereas there exist, especially in the case of compound **10**, delocalized ones. Besides the expected differences, there are some similarities in the orbital constitution of the two ligands since the HOMO – 2 orbital is largely located in the benzoic ring, the HOMO – 3 in the pyridine ring, while the HOMO – 1 orbital extends over the pyridine ring and the neighboring imine bond in both compounds.The LUMO + 2 orbital is mainly located on the pyridine, ring and the LUMO + 1 extends over the benzoic and the carboxylic group. In general the LUMOs appear more delocalized in **10** indicating a less pronounced charge transfer character bands in its spectra relative to **11**.

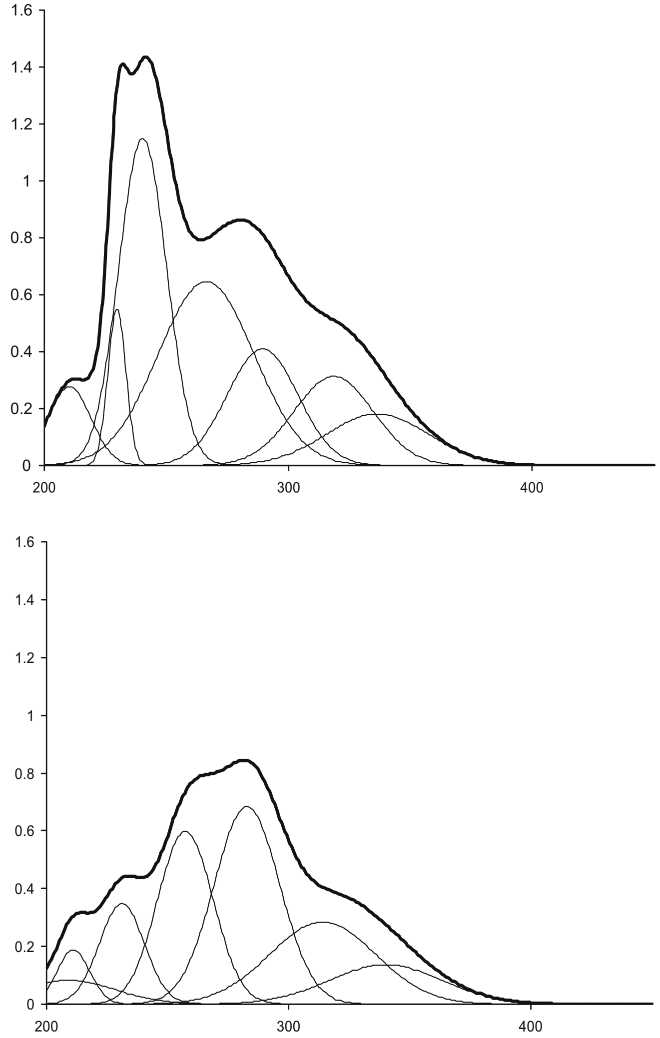

Fig. 3. Electronic excitation spectra of the ligands **10** (above) and **11** (bottom) in dichloromethane. Individual excitations are Gaussian type curves and appear in ordinary line width while the total spectrum is represented by a bold line.

Analogous computations were carried out for the methyl and phenyl derivatives and although there is only limited value in their outcome due to the assumption of only s and p orbitals for the main group metals, their findings reveal limited contribution by the organotin fragment to the above considered frontier MOs. There appears to be only one occupied molecular orbital with Sn character, a fact that is supported by the striking similarity of the organotin compound electronic excitation spectra with the ones of the free ligands.

3.3. Solution NMR data

The study of ^{1}H and ^{13}C NMR spectra in solution and especially the coupling constants of the carbon atoms directly attached to the tin center may serve as an indication of the coordination environment of tin in solution. Since the compounds are soluble in $CDCl_3$ solvolysis is not expected to occur and therefore the spectroscopic information is correlated with the solid state structure of the compounds. In Table 2 there are summarized the most relevant data

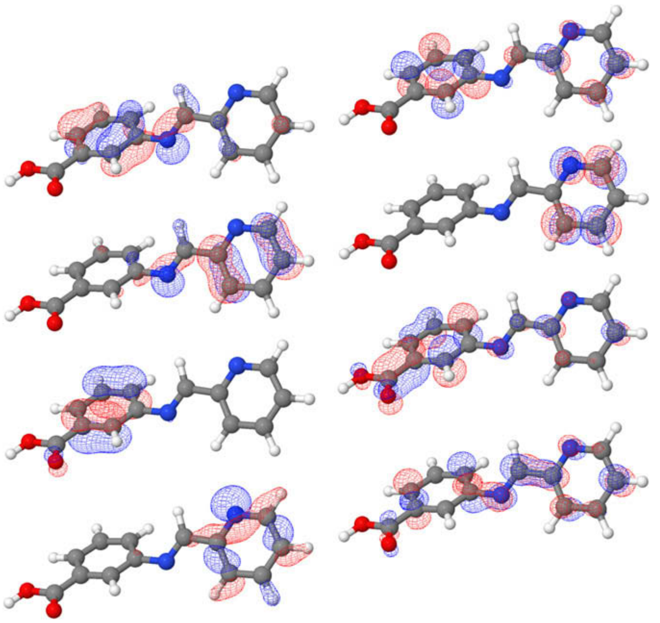

Fig. 4. Frontier molecular orbitals for compound **10**. The HOMOs are on the left and the LUMOs on the right side, while in every case the orbitals are drawn in increasing energy order.

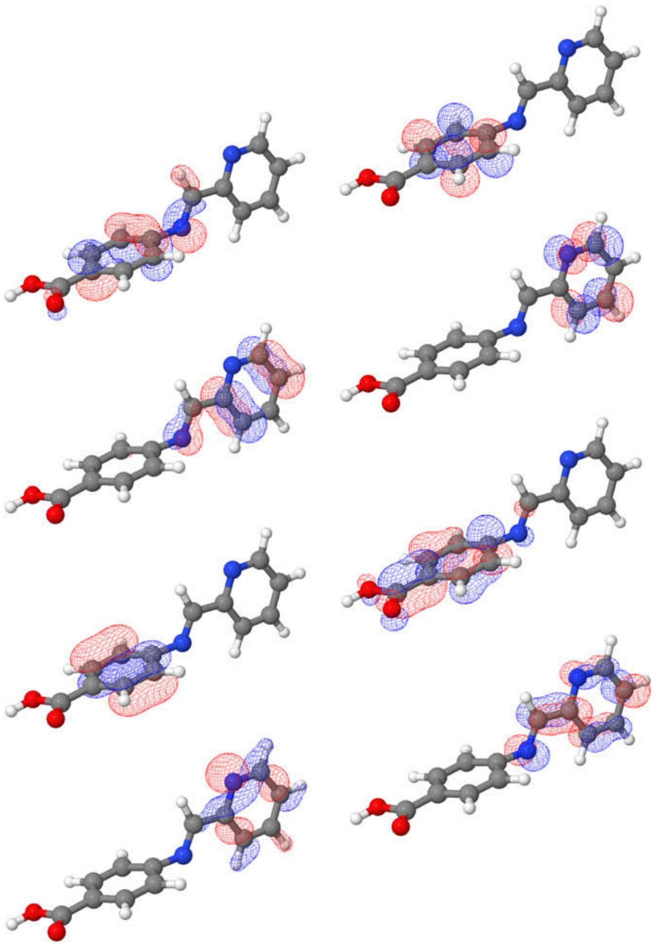

Fig. 5. Frontier molecular orbitals for compound **11** drawn as the corresponding ones of **10** in Fig. 4.

with respect to their aid in the confirmation of the geometry adopted by the compounds in solution.

The NMR data indicate that in solution there is no participation of the imino nitrogen atom in the coordination to tin since there are no appreciable changes in the imine proton and carbon resonances between the free ligands and the organotin compounds. The carboxylate coordination is apparent from the slight but detectable downfield shift of the carboxylate carbon atom [25]. The most relevant information however is extracted from the chemical shift and the coupling constant of the α-carbon atom of the organic substituent and, when possible, from the same observables of the proton of the above carbon atom. The values obtained for the alkyl and benzyl derivatives range well within the limits set for four-coordinate tin since they do not exceed the high limit value 390 Hz [26–28] except in the case of the trimethyl derivatives **7a** and **8a** which, however, are not very far from it. The crystal structure determination of **7a** has revealed the coordination of a water molecule to tin (*vide infra*) and it is unlikely that the water has been removed during the solution in $CDCl_3$ for the spectra recording whereas it was retained throughout the recrystallization procedure which involved treatment in boiling toluene. Note should be taken at this point that it was not possible to observe the coupling in the case of all triphenyl derivatives. For these compounds however the corresponding carbon atom signal was observed at the field strength proposed for tetrahedral tin environment, i.e. around 138 ppm [29]. In the case of **7d** the observed $^{1}J(^{119}Sn-^{13}C)$ coupling constant of 650 is again within the limits 550–670 Hz established in literature.[18] In the methyl and benzyl derivatives it was possible to observe the $^{2}J(^{119}Sn-^{1}H)$ couplings which range between 57 and 71 Hz, being consistently higher for the benzyl derivatives. For this coupling it has been documented that values around 80 Hz indicate octahedral tin, [30] in which case our findings support a coordination number not exceeding five.

3.4. Mössbauer measurements

The Mössbauer spectra of the triorganostannyl esters of carboxylates are more subtle in their interpretation as the range over which the quadrupole splittings are observed may be shifted due to large electronegativity differences between the donor atoms and tin therefore calling again for speculation. In general higher quadrupole splittings, Δ, correspond to higher coordination

Table 2
Relevant ^{1}H and ^{13}C NMR data in $CDCl_3$ solution. Chemical shifts (ppm) are downfield from internal TMS standard and the $^{1}J(^{119}Sn-^{13}C)$ and $^{2}J(^{119}Sn-^{1}H)$ coupling constants (Hz), where observed, following in parentheses.

Compound	C_{carb}[a]	C_{im}	C_{α}	H_{im}	H_{α}
10	167.80	161.90	–	8.63	–
7a	171.06	161.17	−2.35 (395)	8.66	0.65 (57.6)
7b	171.09	161.14	16.55 (369)	8.66	1.36 m[b]
7c	170.85	161.14	33.89 (355)	8.65	1.97–2.05 m[b]
7d	172.44	161.41	138.26 (650)	8.62	–
7e	172.30	160.99	24.43 (310)	8.63	2.68 (68.3)
11	166.90	162.30	–	8.61	–
8a	171.21	161.80	−2.32 (395)	8.58	0.64 (57.2)
8b	171.59	161.65	16.55 (355)	8.59	1.36 m [b]
8c	170.70	161.47	33.53 (342)	8.58	1.91–2.01 m[b]
8d	172.30	161.98	138.37	8.56	–
8e	171.49	161.92	24.19 (319)	8.60	2.68 (70.4)
12	166.60	162.40	–	8.70	–
9a	170.37	161.68	−2.32 (388)	8.69	0.64 (57.2)
9b	169.62	160.70	16.01 (362)	8.71	1.35 m[b]
9c	170.64	161.71	34.04 (337)	8.70	1.97–2.01 m[b]
9d	172.05	161.92	138.21	8.67	–
9e	171.33	161.56	24.12 (328)	8.64	2.68 (68.4)

[a] The subscripts denote carboxylate (carb), imino (im) and the atom of the alkyl or aryl group directly attached to the tin center (α), respectively.

[b] Non-resolved multiplet incorporating more than one types of proton.

numbers, the accepted ranges being 2.0–2.4, 2.6–3.0 and around 3.5 mm s^{-1} for coordination numbers four, five and six, respectively, [31]. Chelate ligands are expected to affect the above ranges since they contribute significantly to the asymmetry of the tin environment [32]. Besides providing grounds for polymeric network formation. In the case of high coordination numbers one may not exclude the participation of the amino substituent to the formation of the tin coordination sphere, a fact that has generally have received little attention. The isomer shift, δ, and the ratio $\rho = \Delta/\delta$ have been used to determine the coordination number of tin and of the asymmetry in it, being directly or indirectly related to the coordinating mode of the ligands present in the tin coordination sphere [33]. The trimethyl derivatives (**7a**, **8a** and **9a**) and a tributyl one (**7b**) are at the borderline of being considered five-coordinated, a fact supported by the infrared spectra and the structure determination for one of them. The single tricyclohexyl derivative studied (**8c**) is certainly tetrahedral with monodentate carboxylate. Tetrahedral environment can also be assigned to the tribenzyl derivatives **8e** and **9e**, the tributyl ones of 4- and 3,5-substituted benzoates (**8b**, **9b**) and to the triphenyl compound **8d**. The occurrence of more than a signal for these compounds suggests a varying degree of secondary interaction from the second carboxylate oxygen in an intermolecular chelating or intramolecular bridging fashion. The triphenyl ester of the disubstituted acid, **9d**, resembles the methyl esters and is expected to be polymeric in nature. The interesting finding is the existence of high coordination number for the phenyl and benzyl esters of the 3- substituted ligand, where there appears to exist some coordination of the pyridine or imine nitrogen to tin (Table 3).

Table 3
Mössbauer spectroscopic data. The line half-widths, the quadrupole splittings and the isomer shifts are reported in mm s^{-1}.

Compound	δ	Δ	ρ (Δ/δ)	$\Gamma_{1/2}$
7a	1.23	3.05	2.48	0.84
	1.59	3.23	2.03	0.68
7b	1.36	3.34	2.46	1.08
	1.88	3.38	1.80	0.70
7d	1.24	2.63	2.12	0.90
	0.61	2.26	3.70	0.90
7e	1.37	1.92	1.40	0.90
	0.65	3.49	5.37	0.90
8a	1.33	3.50	2.63	0.86
8b	1.23	2.87	2.33	0.84
	1.60	2.94	1.84	0.94
8c	1.47	2.68	1.82	0.84
8d	1.16	2.51	2.16	0.90
	1.02	1.70	1.67	0.90
8e	1.39	3.34	2.40	0.88
	1.29	2.48	1.92	0.88
	0.78	1.53	1.96	0.88
9a	1.30	3.39	2.61	0.84
9b	1.42	2.72	1.92	0.90
	1.49	3.54	2.38	0.86
9d	0.98	2.53	2.58	1.04
	1.37	2.72	1.99	0.80
9e	1.04	2.57	2.47	1.02
	1.49	2.95	1.98	1.00

3.5. Crystallographic information

The ORTEP representation of the free acids **10** and **11**, belonging to the $P2_1/c$ space group, is shown in Fig. 6. The crystal structure for the other monoclinic form of **10**, in the C2/c space group, has been reported recently [34]. Whereas in the structures reported here the pyridinylimino benzoic acids are in non-planar conformations, in the C2/c polymorph of **10** the benzene fragment is only slightly twisted relative to the remaining part of the molecule. The twisted conformation can be rationalized as a relieve of a steric hindrance between the –N=CH– group H atom and the neighboring H atoms of the benzene ring at the cost of the conjugation energy of the imino group with the benzene ring. A survey of the Cambridge Crystallographic Database (CSD; [35]) shows 10 crystal structures with 14 (2-pyridylmethylene) benzeneamine fragments that possess H atoms at the α- positions of the benzene ring. The twist angle around the C–N bond between the benzene ring and the imino group ranges from 11° to 43° with the intramolecular H···H contact from 2.03 Å (i.e. nearly equal to the sum of van der Waals radii of H atoms [36]) to the maximum value of 2.49 Å. In the reported crystal structures the twist angle is relatively large, 46.1° and 37.7° for **10** and **11**, respectively, but as shown by the polymorphism of **10**, it is more a result of crystal packing forces than a molecular property. In all molecules with the (2-pyridylmethylene) benzeneamine fragment deposited in the CSD and in molecules **10** and **11** reported here the imino and pyridine N atoms are transoidaly oriented with the twist angle of the pyridine unit relative to the imino group being small and not exceeding 17°.

In both crystalline forms of **10**, the molecules join *via* a typical carboxylic acid–pyridine $R_2^2(8)$ synthon consisting of a strong O–H···N and weak C–H···O interactions [37,38] but there is an interesting difference in the structure of the hydrogen bonded assemblies: in the C2/c form molecules assemble into discrete, nearly planar, centrosymmetric dimers whereas in the $P2_1/c$ form they arrange into helices along the twofold screw axis. The latter organization leads to a more efficient packing as shown by the crystal densities: 1.38 and 1.42 g cm^{-3} for C2/c and $P2_1/c$ polymorphs, respectively. Also in compound **11** the best hydrogen-bond donor, the carboxylic group, interacts with the best hydrogen-bond acceptor, the pyridine N atom, forming a 1D polymeric structure, but in this case a weaker C–H···O interaction is not present.

For compound **7a·H$_2$O**, which is an aqua-trimethyltin ester of the acid 10, two conformational polymorphs, designated as α and β forms, were isolated, both belonging to the monoclinic space group $P2_1/n$. Whereas in both structures the tin environment is similar, the benzoate ligands strongly differ in conformation The tin atoms are in a distorted trigonal bipyramidal environment with the apical positions occupied by one carboxylate oxygen atom and one water molecule whereas methyl groups are located in the

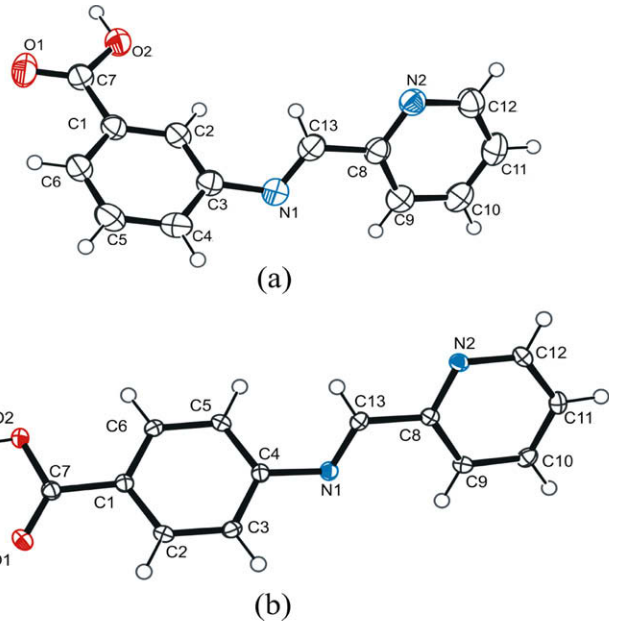

Fig. 6. ORTEP repesentations of the monomers of the free acids **10** (a) and **11** (b).

equatorial plane. The Sn atom deviates 0.16 Å out of this plane in the direction of the carboxylate O atom.

The carboxylate group is clearly monodentate to the tin center and the Sn–O bond lengths of 2.166 and 2.187 Å correlate nicely with the Sn–OH_2 distances, with the sum of the two Sn–O distances in both molecules equal within the experimental error. The coordination geometry around the Sn atom is very similar to that observed in other aqua-trimethyltin carboxylates [39–44]. The details of molecular geometry for **7a**·H_2O are given in Table 4. In the polymorphs of **7a**·**H**$_2$O the pirydyliminobenzoate ligand shows different orientation of the pirydylimine fragment as well as different orientation of the carboxylate ester group as illustrated in Fig. 7. As both polymorphs were isolated from the same crystallization batch, with the polymorph α precipitating first and the polymorph β appearing only later on, the form β should be considered as slightly more stable than α. Additional support is provided by crystal densities of the both forms (Table 5) showing a more dense packing for the β form of **7a**·**H**$_2$O than for the α form. In the two crystal structures water molecules donate hydrogen bonds to the pyridine N atom and the carboxylate non-coordinating O atom to form a two-dimensional polymeric structure. The imine N atom which generally should be a good acceptor for hydrogen bonding is not easily accessible to this interaction as in the flattened ligand conformation the electron pair occupying a sp^2 orbital of the imine nitrogen atom is significantly shielded by the pyridine and benzene hydrogen atoms.

Semi-empirical calculations are not expected to enlighten the structural conformations of the triorganotin compounds studied since they do not treat adequately hypervalent compounds of tin or any other main group metalloid. In view of the experimentally obtained structure of **7a** hydrate we attempted a series of calculations in which the approach of a water molecule to the tin center was considered. In the process it was found obligatory to force the perpendicularity of the three Sn–C bonds relative to the Sn–O of the carboxylate site. When the optimization was carried out in this way, it was possible to obtain final structures with general similarity to the crystallographically obtained one as can be seen in Fig. 8, except for a weak Sn–OH_2 interaction with the computed Sn–O distance converging at around 2.80 Å while the observed one is around 2.40 Å.

However, applying the above approximation to the conformations as they appear in the two polymorphs of the compound isolated they proved to be of approximately equal stability as reflected in their calculated heat of formations which were computed to be −62.242 and −62.612 kJ, respectively, a fact supported by the easy isolation of both conformers by slightly varying the crystallization procedure.

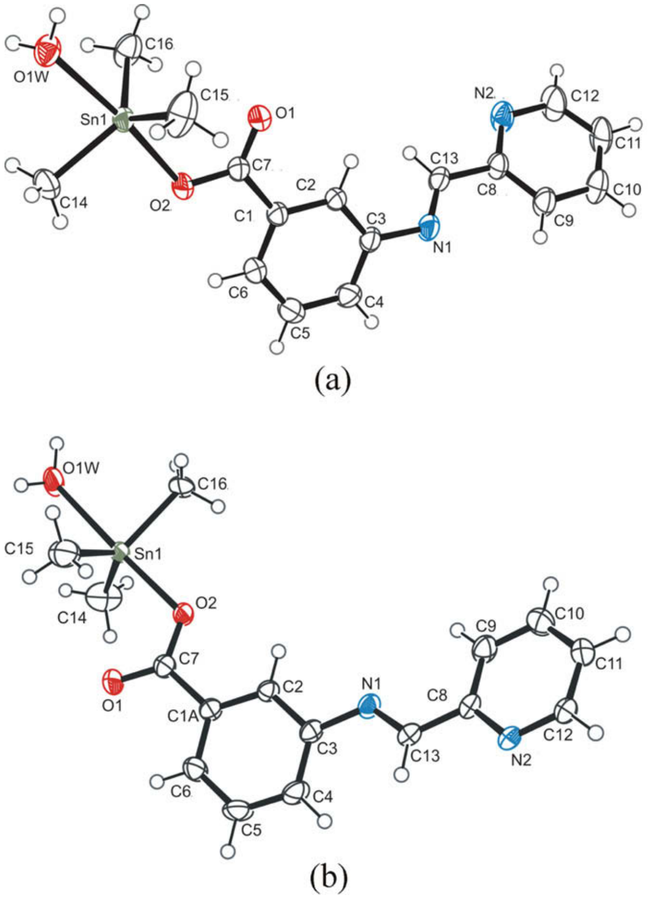

Fig. 7. Molecular structure of **7a**·H_2O in (a) polymorph α and (b) polymorph .

Table 4
Selected bond lengths (Å) and angles (°) for **7a**·H_2O in both polymorphic forms.

Bond/angle	7a·H_2O polymorph α	7a·H_2O polymorph β
Sn–O	2.1877(17)	2.1660(15)
Sn–OH_2	2.3773(19)	2.3974(19)
Sn–C[a]	2.111(3)	2.106(3)
	2.114(3)	2.099(2)
	2.123(3)	2.107(3)
O–C	1.290(3)	1.287(3)
O′–C[b]	1.234(3)	1.232(3)
O–Sn–C	95.91(10)	92.03(8)
	90.95(10)	95.10(10)
	95.69(10)	95.65(10)
H_2O–Sn–C	87.39(10)	85.79(8)
	83.47(10)	84.59(11)
	86.37(10)	86.70(12)
H_2O–Sn–O	174.38(7)	177.32(7)
O–C–O′	123.8(2)	124.5(2)

[a] The carbon atoms bonded to tin are not identified but all observed values are listed.

[b] Superscript used to define the non-bonding oxygen in the triorganotin compounds.

3.6. Emission data

Emission spectra of the pyridinylimino benzoic acids were recorded both in the solid state and in methanol solution following an excitation at 324 nm. In the solid state the three compounds reveal emission at almost at identical wavelengths, with small intensities **12** presenting the lower and **11** the higher one. This is due to the polymeric nature of the compounds as the X-ray structure determination revealed. In methanol solution however, where the corresponding monomers are the predominant species, the excited states differ significantly and the emissions recorded show maxima at 456 nm for **12**, 430 nm for **10** and 390 nm for **11**, while the relative intensities are two orders of magnitude larger than in the solid state and increasing in the given order.

Preliminary measurements for the organostannyl esters in methanol, following excitation at 324 nm reveal the fact that although the 3-substituted derivatives emit at longer wavelengths, the relative emission intensity is reversed in their favor with respect to their 4-substituted counterparts, while the substitution at tin does not affect significantly the emission maximum. The observed emission, on the other hand is by an order of magnitude less than the one recorded for the free ligands.

4. Conclusion

Triorganostannyl esters of pyridinyliminobenzoates can be synthesized by two routes giving organotin compounds with a

Table 5
Crystallographic details for the studied compounds.

	10	**11**	**7a**·H_2O polymorph α	**7a**·H_2O polymorph β
CCDC	739745	739746	739747	739748
Formula	$C_{13}H_{10}N_2O_2$	$C_{13}H_{10}N_2O_2$	$C_{16}H_{20}N_2O_3Sn$	$C_{16}H_{20}N_2O_3Sn$
Wavelength	Mo Kα	Mo Kα	Mo Kα	Mo Kα
Mr (g mol^{-1})	226.23	226.23	407.03	407.03
Crystal system	Monoclinic	Monoclinic	Monoclinic	Monoclinic
Space group	$P2_1/c$	$P2_1/c$	$P2_1/n$	$P2_1/n$
Temperature [K]	293	100	130	130
a [Å]	10.8012(5)	3.7588(1)	6.5874(3)	11.3719(3)
b [Å]	7.4645(4)	18.2354(4)	23.9532(19)	8.3578(2)
c [Å]	13.1830(5)	15.3571(5)	11.425(3)	18.3187(6)
β [°]	92.461(4)	92.098(3)	95.957(11)	90.881(3)
V [$Å^3$]	1061.91(9)	1051.92(5)	1793.0(4)	1740.88(8)
Z	4	4	4	4
ρ_{cald} (g cm^{-3})	1.415	1.428	1.508	1.553
$\mu(Mo_{K\alpha})$ (mm^{-1})	0.098	0.099	1.437	1.480
Measured reflns	8259	12650	17404	18518
Independent reflns	2159	2153	3657	3766
Observed reflns	1338	1949	3098	3021
Refined parameters	158	159	207	209
$R1$ ($R1$ all data)	0.0339 (0.0687)	0.0324 (0.0357)	0.0219 (0.0296)	0.0201 (0.0339)
$wR2$ ($wR2$ all data)	0.0785 (0.0938)	0.0806 (0.0829)	0.0505 (0.0534)	0.0434 (0.0524)
Max. and min. [e $Å^{-3}$]	0.15, −0.18	0.28, −0.19	0.84, −0.36	0.97, −0.50

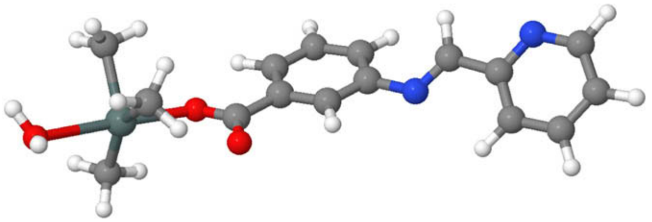

Fig. 8. Computed structure for **7a** hydrate by PM6. Structures drawn using the Jmol program [45].

potential diimine coordinating site. The ligands form supramolecular structures in the solid state with extensive intermolecular hydrogen bonding and readily coordinate to triorganotin sites through the carboxylate group. Solid state interactions are also present in the organotin carboxylates giving rise to a variety of local and overall structures and the occurrence of more than one local tin environment as IR and Mössbauer data indicate. Crystal structure determination for a methyl derivative determined, besides its existence as a hydrate, the presence of two discrete polymorphs differing in the relative orientation of the carboxylate towards the imino group. Inspection and analysis of the UV–vis spectra of the ligands and the organotin compounds indicate the occurrence of bands with appreciable charge transfer character which may facilitate the use of the compounds as metalloligands towards transition metals with possible tuning of the final heterodimetallic system's photophysical and photochemical properties.

Appendix A. Supplementary data

Supplementary data associated with this article can be found, in the online version, at doi:10.1016/j.molstruc.2009.11.038.

References

[1] A. Vlcek Jr., Coord. Chem. Rev. 230 (2002) 225–242. and references therein.
[2] R.S. Herrick, C.J. Ziegler, H. Bohan, M. Corey, M. Eskander, J. Giguere, N. McMicken, I. Wrona, J. Organomet. Chem. 687 (2003) 178–184. and references therein.
[3] B.P. Buffin, E.B. Fonger, A. Kundu, Inorg. Chim. Acta 355 (2003) 340–346.
[4] B.P. Buffin, P.J. Squattrito, A.O. Ojewole, Inorg. Chem. Commun. 7 (2004) 14–17.
[5] R. Garcia-Rodriguez, D. Miguel, Dalton Trans. (2006) 1218–1225.
[6] I. Omae, Appl. Organometal. Chem. 17 (2003) 81–105. and references therein.
[7] E.R.T. Tiekink, Trends Organomet. Chem. 1 (1995) 71–116.
[8] S. Chowdhury, G.K. Patra, M.G.B. Drew, N. Chattopadhyay, D. Datta, J. Chem. Soc., Dalton Trans. (2000) 235–237.
[9] E.C. Riesgo, Y.Z. Hu, R.P. Thummel, D.V. Scaltrito, G.J. Meyer, Inorg. Chem. 40 (2001) 3413–3422.
[10] D.R. McMillin, K.M. McNett, Chem. Rev. 98 (1998) 1201–1220.
[11] S.D. Ittel, L.K. Johnson, M. Brookhart, Chem. Rev. 100 (2000) 1169–1204.
[12] D. Tzimopoulos, M. Gdaniec, T. Bakas, P.D. Akrivos, J. Coord. Chem. 62 (2009) 1218–1231.
[13] Oxford Diffraction, Crysalis CCD and RED, ver. 1.171.31, Oxford Diffraction, Abingdon, Oxfordshire, UK, 2006.
[14] G.M. Sheldrick, Acta Crystallogr. A64 (2008) 112–122.
[15] L.J. Farrugia, J. Appl. Crystallogr. 30 (1997) 565.
[16] C.F. Macrae, P.R. Edgington, P. McCabe, E. Pidcock, G.P. Shields, R. Taylor, M. Towler, J. van de Streek, J. Appl. Cryst. 39 (2006) 453–457.
[17] G.K. Sandu, S.P. Verma, L.S. Moore, R.V. Parish, J. Organomet. Chem. 321 (1987) 15–25.
[18] F.P. Pruchnik, M. Banbula, Z. Ciunik, M. Latocha, B. Skop, T. Wilczok, Inorg. Chim. Acta 356 (2003) 62–68.
[19] T.S. Basu Baul, R. Wandondor, E. Rivarola, C. Pettinari, A. Linden, J. Organomet. Chem. 690 (2005) 1413–1421.
[20] Z. Rzaczynska, R. Mrozek, J. Lenik, M. Sikorska, T. Glowiak, J. Chem. Crystallogr. 30 (2000) 519–524.
[21] J.J.P. Stewart, J. Mol. Mod. 13 (2007) 1173–1213.
[22] MOPAC2009, James J.P. Stewart, Stewart Computational Chemistry, Colorado Springs, CO, USA, 2008. Available from: <http://OpenMOPAC.net>.
[23] Systat Software Inc. Peakfit program version 4.11.
[24] AFS client-server computational environment of the Aristotle University of Thessaloniki.
[25] M. Nath, R. Yadav, Bull. Chem. Soc. Jpn. 71 (1998) 1355–1362.
[26] J. Holeček, M. Nadvornlk, K. Handllr, A. Lyčka, J. Organomet. Chem. 241 (1983) 177–184.
[27] M. Nadvornik, J. Holeček, K. Handllr, A. Lyčka, J. Organomet. Chem. 275 (1984) 43–51.
[28] A. Lyčka, J. Holeček, M. Nadvornlk, K. Hadler, J. Organomet. Chem. 280 (1985) 323–329.
[29] A. Lyčka, M. Nadvornlk, K. Handllr, J. Holeček, Collect. Czech. Chem. Commun. 49 (1984) 2903–2911.
[30] H.C. Clark, V.K. Jain, R.C. Mebrotra, B.P. Singh, G. Srivastava, T. Birchall, J. Organomet. Chem. 279 (1985) 385–394.
[31] R. Willem, A. Bouhdid, B. Mahieu, L. Ghys, M. Biesemans, E.R.T. Tiekink, D. de Vos, M. Gielen, J. Organomet. Chem. 531 (1997) 151–158.
[32] L.C.M. Costa, J.R.daS. Maia, G.M. de Lima, J.D. Ardisson, Solid State Commun. 137 (2006) 376–380.
[33] G. Eng, X. Song, A. Zapata, A.C. de Dios, L. Casabianca, R.D. Pike, J. Organomet. Chem. 692 (2007) 1398–1404. and references therein.
[34] Q. Wang, Y.-Y. Sun, D.-Q. Wang, Acta Crystallogr. E63 (2007) o4597.
[35] F.H. Allen, Acta Crystallogr. β58 (2002) 380–388.
[36] A. Bondi, J. Phys. Chem. 68 (1964) 441–451.
[37] T.R. Shattock, K.K. Arora, P. Vishweshwar, M.J. Zaworotko, Cryst. Growth Des. 8 (2008) 4533–4545.
[38] J.A. Bis, P. Vishweshwar, D. Weyna, M.J. Zaworotko, Mol. Pharm. 4 (2007) 401–416.
[39] C. Ma, J. Li, R. Zhang, D. Wang, Inorg. Chim. Acta 359 (2006) 2407–2416.

[40] F. Ahmad, S. Ali, M. Parvez, A. Munir, M. Mazhar, K.M. Khan, T.A. Shah, Heteroat. Chem. 13 (2002) 638–649.

[41] M. Parvez, S. Ali, M. Mazhar, M.H. Bhatti, M.N. Khokhar, Acta Crystallogr. C55 (1999) 1280–1282.

[42] C. Ma, J. Li, R. Zhang, D. Wang, J. Organomet. Chem. 691 (2006) 1713–1721.

[43] H.-Y. Wang, H.-D. Yin, D.-Q. Wang, Acta Crystallogr. E63 (2007) o1226–o1227.

[44] T.I. Ovsetsina, N.G. Furmanova, E.V. Chuprunov, V.I. Shcherbakov, Kristallografiya (Russ.) 38 (1993) 71–76.

[45] Jmol: an open-source Java viewer for chemical structures in 3D. Available from: <http://www.jmol.org/>.